Peris Pérez, B.; Navarro Esbri, J.; Molés Ribera, F.; González, M.; Mota Babiloni, A. (2015). Experimental characterization of an ORC (organic Rankine cycle) for power and CHP (combined heat and power) applications from low grade heat sources. Energy. 82:269-276. doi:10.1016/j.energy.2015.01.037.

Experimental characterization of an Organic Rankine Cycle (ORC) for power and Combined Heat and Power (CHP) applications from low grade heat sources

Bernardo Peris[*, a], Joaquín Navarro-Esbrí[a], Francisco Molés[a], Manuel González[b], Adrián Mota-Babiloni[a, c]

[a] ISTENER Research Group. Department of Mechanical Engineering and Construction, Campus de Riu Sec s/n, University Jaume I, E12071, Castellón, Spain.

[b] Expander-Tech, Campus de Riu Sec s/n, University Jaume I, E12071, Castellón, Spain.

[c] Institute for Industrial, Radiophysical and Environmental Safety, Camino de Vera s/n, Polytechnic University of Valencia, E-46022 Valencia, Spain.

Abstract

An Organic Rankine Cycle (ORC) module, designed and built for a specific Combined Heat and Power (CHP) application, is tested in this paper. The aim of the work is to characterize the system performance in the operating range allowed by the ORC. For this purpose, a test procedure has been conducted in a test bench. The heat source has been simulated through a natural gas boiler and a thermal oil heat transfer loop to control the temperature in the low grade range of 90 ºC to 150 ºC. The heat sink has been developed using a dry cooler to control the hot water temperature in the range of 30 ºC, corresponding to a power application, to 80 ºC, of a small-scale CHP application that provides hot water at 90 ºC. Thereby, the results show that the thermal power captured by the ORC, electricity and useful heat produced, increase with the rise of the thermal oil temperature and larger pressure ratios. Moreover, the expander electrical isentropic effectiveness is maximized about 70% for a pressure ratio suitable for a CHP system. The cycle efficiency slightly continues increasing for higher pressure ratios, up to a net electrical efficiency of about 8%.

Keywords: Organic Rankine Cycle (ORC); Combined Heat and Power (CHP); test bench; heat recovery; energy efficiency.

[*] Corresponding Author:
Tel: +34 964728137; fax: +34 964728106.
E-mail address: bperis@uji.es

Nomenclature	
c_p	specific heat capacity ($kJ \cdot kg^{-1} \cdot K^{-1}$)
h	enthalpy ($kJ \cdot kg^{-1}$)
$\dot{m}$	mass flow rate ($kg \cdot s^{-1}$)
P	pressure (bar)
Q	thermal power (kW)
T	temperature (ºC)
U	uncertainty
$\dot{V}$	volumetric flow rate ($m^3 \cdot s^{-1}$)
W	electrical power (kW)
Greek symbols	
ε	effectiveness (%)
η	efficiency (%)
ρ	density ($kg \cdot m^{-3}$)
Subscripts	
e	expander
el	electrical
g	gross
HRVG	heat recovery vapor generator
ise	isentropic
n	net
oil	thermal oil
p	pump
th	thermal
w	water-ethylene glycol mixture
wf	working fluid

1. Introduction

The Organic Rankine Cycle (ORC) has been proven as an efficient way for power generation from low grade heat sources [1]. It is a similar power cycle to the steam Rankine cycle, but uses more volatile fluids instead of water to improve the efficiency in low temperature applications [2]. Its operating principle consists of capturing the thermal energy from the heat source through the evaporation of the working fluid and reducing the enthalpy in an expander to produce mechanical work, which is turned into electricity by an electric generator. This is a closed system, which condenses the vapor from the expander outlet and pressurizes the liquid to restart the cycle again. So, it is considered a simple cycle that requires little maintenance, compared to other power cycles like Kalina [3], Goswami, transcritical cycle or trilateral-flash cycle [4]; in addition to its mature and proven technology against direct conversion techniques (thermo-electric, thermionic or piezoelectric) [5].

The ORC use is mainly focused on renewable heat sources and waste heat recovery applications, like: solar thermal [6], geothermal [7], oceanic [5], biomass [8], Combined Heat and Power (CHP) [9], waste heat from power systems [10], waste heat from industrial processes [11] or other. And therefore, it can contribute to achieve great energy, environmental and economic benefits [12].

This wide range of possibilities has motivated researchers' efforts in order to provide suitable ORC solutions. Thus, various experimental studies have been carried out for different applications, working fluids and expander technologies. In this way, Zhou et al. [13] tested an ORC for waste heat recovery from flue gas, using the working fluid R123 and a scroll expander. The heat source was simulated through a liquefied petroleum gas stove to control the temperature in the range of 90-220 ºC. Thereby, a maximum expander power output of 0.645 kW and cycle efficiency of 8.5% were achieved. Qiu et al. [14] experimented with a biomass-pellet boiler and an ORC for micro-CHP applications, by heating to 46 ºC the cooling water of the condenser outlet. The main working fluid used was HFE7000 and a vane type of expander. So, 0.861 kW were generated with a gross electrical efficiency of 1.41%. Pei et al. [15] constructed and tested a small-scale ORC, using a specially designed turbine and R123 as working fluid. The results showed that a cycle efficiency of 6.8% could be obtained with a temperature difference of about 70 ºC between hot and cold sides. Wang et al. [16] tested a low temperature solar ORC using R245fa as working fluid and a rolling-piston as expander. The results showed an average shaft power output of 1.64 kW and an overall power generation efficiency that ranged between 3.2-4.2%, depending on the solar collector used. Manolakos et al. [17] demonstrated the technical feasibility of a low-temperature solar ORC for reverse osmosis desalination. The working fluid used was R134a and a scroll expander obtained from a compressor in reverse operation. So, the results showed net mechanical efficiencies ranging from 0.73% to 1.17%. Moreover, the researchers pointed the direct influence of the expander effectiveness on the cycle efficiency.

Taking into account this influence of the expander on the cycle efficiency, many researchers focused on its improvement to achieve more efficient systems. In this way, Clemente et al. [18] demonstrated, using a numerical model, that through an expander with a higher built-in volume ratio (Vi) the entire useful operational field of the expander moves toward higher pressure ratios, that could be effectively exploited in more efficient ORCs. Moreover, pointed the regenerative cycle configuration as a mean to achieve higher benefits in electrical efficiency. In this way, Peris et al. [] tested an ORC with the regenerative cycle configuration, R245fa as working fluid and an expander with a high Vi of 8.0 for power applications from low grade heat sources. The results showed that the electrical isentropic effectiveness of the expander was maximized about 65% for a pressure ratio around 7. So, a gross electrical efficiency of 12.32% was obtained for a heat source temperature about 155 ºC and a direct dissipation to the ambient. An ORC also with the regenerative cycle configuration, the working fluid R123 and a scroll expander with a Vi of 4.57, was tested by Peterson et al. [19]. The results showed a gross mechanical cycle efficiency of 7.2% and an expander mechanical isentropic effectiveness ranging between 45-50%. Lemort et al. [20] presented the results of an experimental study carried out on a prototype of an open-drive oil-free scroll expander, which was integrated into an ORC using R123. The researchers demonstrated that for low pressure ratios in the expander, lower than the imposed by the Vi of 4.05, it operates in over-expansion with low effectiveness. However, with a suitable pressure ratio the expander achieved a maximum mechanical isentropic effectiveness of 68%. Declaye et al. [21] characterized an oil-free scroll expander, with a Vi of 3.95, in an ORC with R245fa as working fluid. The operating parameters varied during tests included expander pressures and rotational speed. Thereby, a maximum mechanical isentropic effectiveness in the expander of 75.7%, shaft power of 2.1 kW and mechanical cycle efficiency of 8.5% were obtained. Moreover, up to 50 ºC of hot water was produced from the condenser outlet, as a CHP system. Bracco et al. [22] reported that in the literature the usual

expander effectivenes ranges between 60-65% with peaks of 68-70%, that are in compliance with their results. The researchers tested a small-size ORC prototype using the working fluid R245fa and a scroll expander adapted from a commercial HVAC. In their study it can be seen that the expander operates in under-expansion, a pressure ratio higher than the imposed by the Vi of the expander. Therefore, the maximum expander effectiveness was achieved for the lowest expansion ratio, obtaining a net electrical cycle efficiency around 8%. Kang [23] designed a radial turbine for its application, with a pressure ratio of 4.11, to directly operate connected to a high-speed synchronous generator and to use R245fa as working fluid. Thereby, the results showed a maximum electrical efficiency of 5.22%, turbine electrical isentropic effectiveness of 78.7% and electrical power of 32.7 kW. Kane et al. [24] introduced the concept of a mini-hybrid solar power plant integrating a field of solar concentrators, two superposed ORCs and a (bio-) diesel engine. Regarding to ORC, it was pointed the limitation of the scroll expander, modified from a standard compressor, on the limited pressure range and Vi for an efficient operation. Hence, proposed to use two superposed ORCs, each one with an optimized working fluid and expander to operating conditions. So, the working fluids selected were R123 for the topping ORC and R134a for the bottoming ORC, both with scroll expanders with a Vi of 2.3. Thereby, the results showed that the superposed cycle achieved a net electrical efficiency upper 12% during tests.

From the reviewed information, it can be seen that the cycle efficiency is the main parameter assessed with the aim to improve it. It is justified in that, for a given thermal power in the heat source of a specific application, a higher electrical benefit can be reached, which plays a key role on a project feasibility [25]. In this way, it has been pointed the high influence of the expander on the cycle efficiency, that commonly is referred to volumetric machines due to result cost effective for low temperature applications [26]. Furthermore, an appropriate operating pressure ratio in the expander, a suitable working fluid and an efficient cycle configuration are also recommendations to increase the electrical gain of a specific application.

Taking this into consideration, this work focuses on the performance analysis of a commercial ORC module

~~Taking this into consideration, in this work a commercial ORC module that uses a volumetric expander, R245fa as working fluid and a regenerative cycle configuration is tested in the complete operating range allowed by the system. Therefore, despite the commercial ORC module was designed and built for a specific small-scale CHP application, both power and CHP applications are going to be addressed in a range of temperatures corresponding to low grade heat sources. Thereby, this work contributes with a deep thermodynamic analysis of actual performance data of a commercial ORC module operating for power and CHP form low grade heat sources.~~

~~Thereby, this work contributes to a deep analysis of experimental performance data of an actual ORC, which is tested in a wide operating range for low temperature applications.~~

For this purpose, the rest of the paper is organized as follows. Section 2 describes the test bench used. Section 3 shows the methodology employed, pointing the measuring devices used, equations for the thermodynamic analysis and test procedure. Section 4 presents and discusses

the results of the system characterization. And finally, section 5 summarizes the main conclusions of the work.

2. Test bench description

In order to conduct the system performance characterization a monitored test bench has been used and adapted to the planned operating conditions. So, the main parts of this facility are addressed.

2.1. Heat source

A low grade heat source has been simulated using a natural gas boiler and a thermal oil heat transfer loop, as it can be appreciated in Fig.1.a. The facility allows to supply the thermal power demanded by the ORC, besides to control the test conditions. For this, it is composed of two loops. The first one is the loop of the boiler, which is automatically adjusted to the thermal power demand, while the second one allows to vary the volumetric flow rate that enters in the ORC, through a pump frequency inverter, and to control the inlet temperature in the ORC, using a three way valve and a PID controller.

The basic scheme of the facility is shown in Fig.1.b, whose main components are: 1-natural gas boiler, 2-ORC, 3-centrifugal pumps, 4-three way valve, 5-expansion tank, 6-main safety valve.

Fig. 1. Heat source test bench: (a) general view of the facility, (b) basic scheme.

2.2. Heat sink

With the aim to characterize the system performance along power and CHP applications, a heat sink facility has been adapted to operate in the planned conditions. The facility can be appreciated in Fig.2.a along with the ORC module during tests. It is based on a dry cooler, located on the cover of the industrial building as shows Fig.2.b, and a heat transfer loop with a mixture of treated water and 20% of ethylene glycol. Thereby, the heat dissipation conditions and, consequently, the ORC condensation conditions can be controlled. For this, it uses a PID controller that adjusts the dry cooler fans velocity according to the hot water inlet temperature in the ORC and a frequency inverter in the pump to set the volumetric flow rate.

The basic scheme of that facility is illustrated in Fig.2.c, whose main components are: 1-dry cooler, 2-ORC, 3-centrifugal pump, 4-deaerator, 5-membrane expansion vessel, 6-safety valve.

Fig.2. Heat sink test bench: (a) general view of the facility and ORC module, (b) dry cooler, (c) basic scheme.

2.3 ORC module

The ORC used in this work is a commercial module from Rank® [27]. This ORC uses a regenerative cycle configuration that allows not only recovering the thermal energy from the heat source, but also the waste heat from the expander outlet to preheat the liquid, improving the cycle electrical efficiency. Regarding to design issues, the module can generate an electrical power up to 45 kW, which is determined by the electric generator rated power. The rated thermal power is determined by the heat exchangers dimensions, which were designed to recover up to 450 kW from the heat source and to provide up to 400 kW of useful heat.

These and other design parameters of the ORC module are listed in Table 1.

Table 1. Rank® ORC module parameters.

3. Methodology

In this section the main measuring devices used for the system motoring, equations for the experimental data analysis and test procedure conducted are addressed.

3.1. System monitoring

Focusing on the ORC monitoring, the main parameters measured and registered are represented in Fig. 3. In the first place, the thermal power is monitored in the hot side through inlet and outlet thermal oil temperatures, using surface thermocouples, and volumetric flow rate, using a vortex flow meter. The useful heat produced by the ORC is monitored in the cold side through inlet and outlet hot water temperatures, using surface thermocouples, and volumetric flow rate, using an electromagnetic flow meter. Within the ORC, the electrical power output from the electric generator is measured using a wattmeter, as well as the electrical pump consumption. Moreover, the expander is monitored through pressure transmitters at the inlet and outlet ports and surface thermocouples at the HRVG, for the working fluid mass flow rate calculations.

Fig.3. Regenerative ORC scheme and main parameters monitored.

The measuring devices uncertainty, extracted from manufacturers' data sheets, and the calculated parameters uncertainties U_y, obtained as a function of the uncertainty on each measured variable U_{x_i} by Eq. (1) [20], are collected in Table 2.

$$U_y = \sqrt{\sum_{i=1}^{N} \left(\frac{\partial y}{\partial x_i} \right)^2 \cdot U_{x_i}^2} \tag{1}$$

Table 2. Uncertainties of measured and calculated parameters.

3.2. Thermodynamic analysis equations

For the analysis of the experimental data obtained during tests various equations have been used. Firstly, the thermal input is calculated through Eq. (2) and thermal oil properties at the operating conditions.

$$Q_{in} = \rho_{oil,out} \cdot \dot{V}_{oil,out} \cdot c_{p\,oil} \cdot \left(T_{oil,in} - T_{oil,out} \right) \tag{2}$$

Similar than thermal input, the useful heat produced by the ORC is quantified using Eq. (3) and water-ethylene glycol mixture properties.

$$Q_{out} = \rho_{w,in} \cdot \dot{V}_{w,in} \cdot c_{p\,w} \cdot \left(T_{w,out} - T_{w,in} \right) \tag{3}$$

The ratio between the useful heat produced and the thermal power input can be defined as the thermal efficiency by Eq. (4). The gross electrical power from the electric generator is directly

measured, as well as the electrical pump consumption and, therefore, it can be obtained the net power output generated using Eq. (5). The electrical efficiency of the cycle can be obtained using the gross electrical efficiency by Eq. (6), and net electrical efficiency by Eq. (7).

$$\eta_{th} = \frac{Q_{out}}{Q_{in}} \tag{4}$$

$$W_n = W_g - W_p \tag{5}$$

$$\eta_g = \frac{W_g}{Q_{in}} \tag{6}$$

$$\eta_n = \frac{W_n}{Q_{in}} \tag{7}$$

Regarding to the expander, the electrical isentropic effectiveness is defined as the relationship between the electrical power measured in the electric generator and the maximum that could be ideally obtained by Eq. (8). For this, it is used the working fluid mass flow rate, calculated by Eq. (9), and a working fluid properties database [28].

$$\varepsilon_{el,ise} = \frac{W_g}{\dot{m}_{wf} \cdot \left(h_{e,in} - h_{e,out,ise}\right)} \tag{8}$$

$$\dot{m}_{wf} = \frac{Q_{in}}{h_{e,in} - h_{HRVG,in}} \tag{9}$$

Other parameters calculated and used for the analysis are the pressure ratio in the expander, defined by Eq. (10), and Carnot efficiency, as Eq. (11) with temperatures in Kelvin units.

$$pressure\ ratio = \frac{P_{e,in}}{P_{e,out}} \tag{10}$$

$$Carnot\ efficiency = 1 - \frac{T_{w,in}}{T_{oil,in}} \tag{11}$$

3.3. Test procedure

In order to test a wide range of low grade heat sources, the thermal oil inlet temperature is controlled in each test from 90 ºC to 150 ºC, while the thermal oil volumetric flow rate is imposed by the pump. On the other hand, for each thermal oil temperature, the hot water temperature is modified between 30 ºC to 80 ºC, while the pump velocity is maintained with a fixed frequency, which was adopted to limit the maximum hot water outlet temperature to 90ºC.

Some restrictions were also considered during tests. So, a minimum temperature difference of 50 ºC was adopted between the thermal oil inlet temperature and hot water inlet temperature to

ensure a minimum pressure ratio. Moreover, a maximum electrical power about 40 kW was established as a test limit.

As a result, 22 steady state points were achieved during tests, which are represented in Fig. 4 according to the controlled variables mentioned, thermal oil and water inlet temperatures. In order to clarify, this and the following figures have been organized in series with respect to the thermal oil temperature, as the legends represent.

The process of selecting steady state consists of taken a time period of 15 min, with a sample period of 1 s, in which the measured parameters are within a fluctuation range lower than 1% on each variable. Once a steady state is achieved (with 900 direct measurements), the data measured are obtained averaging over a time period of 10 min (600 direct measurements).

The operating range registered for each variable during tests is listed in Table 3.

Fig.4. Operating points obtained during steady states in tests.

Table 3. Operating range of each variable obtained during tests.

4. Results and discussions

From the experimental data obtained during tests an analysis has been conducted, whose results are exposed and discussed in this section.

In a first step, the thermal power characterization is addressed. Fig. 5.a shows that the thermal power captured by the ORC increases with the thermal oil inlet temperature. Furthermore, in Fig. 5.b it is noted that, for a specific thermal oil inlet temperature, the thermal power captured also increases for larger pressure ratios.

When the ORC is used in a CHP application the useful heat plays a key role. In this way, Fig. 5.c shows that the thermal power output directly depends on the thermal power input. More detailed, Fig. 5.d shows that the thermal power output increases with the thermal oil inlet temperature, but also for lower hot water temperatures and, consequently, higher pressure ratios. On the other hand, regarding to the thermal efficiency it must be mentioned that, despite its considerable uncertainty, its average value approximates to 90%, which is an indicative of the great energy benefit that could be reached in a CHP application.

Fig.5. Thermal power characterization: (a) thermal oil inlet temperature, (b) pressure ratio, (c) useful heat, (d) hot water inlet temperature.

Now the electrical power characterization is addressed. So, Fig.6.a shows that higher thermal oil temperatures allow higher electrical power outputs. Moreover, it highlights that, for a given thermal oil inlet temperature, the gross electrical power increases with the thermal power captured, which also is related to the pressure ratio as Fig. 6.b represents. Similarly, Fig. 6.c and Fig.6.d show that the net electrical power also increases with the thermal oil inlet temperature, thermal power captured and larger pressure ratios.

Fig.6. Electrical power characterization: (a) gross electricity with thermal input, (b) gross electricity with pressure ratio, (c) net electricity with thermal input, (d) net electricity with pressure ratio.

Regarding to efficiencies, Fig.7.a represents the gross electrical efficiency of the cycle. It is observed that the efficiency tendency quickly grows with the pressure ratio, with a maximum of 9.40%. However, although the pressure ratio continues growing the efficiency tendency seems attenuated. So, if the net electrical efficiency is compared to the Carnot efficiency, in Fig. 7.b, it can be seen that theoretically it should continue to grow, but a technical constraint is presented in the cycle limiting the maximum net electrical efficiency about 8%. This effect can be justified observing Fig. 7.c referred to the expander. So, the electrical isentropic effectiveness of the expander results maximized about 70%, similar to the literature [22], for a pressure ratio, between 2-3, suitable for a small-scale CHP system or a low temperature power application operating with a moderate pressure ratio. This figure also shows the energy losses produced when the expander operates in under-expansion and, still more, in over-expansion. Other energy losses that contribute to draw this curve are heat losses during expansion, frictions, supply pressure drop, internal leakages [29], or the alternator electrical efficiency operating at partial loads [30]. Furthermore, if the gross electrical efficiency of the cycle is compared with the expander electrical isentropic effectiveness, as shows Fig. 7.d, it can be noted that operating with a moderate under-expansion the cycle efficiency can be improved, similar as results of Declaye et al. [21]. Although an excessive under-expansion could deteriorate the cycle efficiency, as reported Clemente et al. [18], requiring in that case an expander with a higher Vi to operate efficiently.

Fig.7. Thermodynamic efficiencies characterization: (a) gross, (b) net, (c) expander, (d) cycle.

5. Conclusions

This work has conducted an experimental characterization of an ORC module in the complete operating range allowed by the system. For this, a test procedure has been conducted, simulating a low grade heat source in the range of 90-150 ºC and a heat sink in the range of 30-80 ºC. So, 22 steady state points have been achieved and analysed.

Thereby, the results show that, for a given ORC module, a higher thermal power can be captured through higher thermal oil temperatures and larger pressure ratios, besides to produce more useful heat. However, for a specific heat source temperature, the useful heat temperature is reduced as the pressure ratio increases, due to the direct relationship between the cycle condensing pressure and the hot water temperature. So, a maximum thermal power input of 390 kW, maximum thermal power output of 350 kW and hot water outlet temperature of 90 ºC have been achieved.

The gross and net electrical powers are enhanced for higher thermal oil temperatures, larger pressure ratios and, consequently, for a higher thermal power captured. So, a maximum gross electrical power of 36.58 kW and net electrical power of 30.91 kW are reached.

The cycle efficiency has demonstrated that grows with the pressure ratio, up to a gross electrical efficiency of 9.40% and net electrical efficiency of 7.92%, while the electrical isentropic effectiveness of the expander is maximized about 70% for a pressure ratio between 2-3, suitable for a small-scale CHP application or a very low temperature power application. Moreover, a comparison between the gross electrical efficiency of the cycle and the expander electrical isentropic effectiveness reveals that operating with a pressure ratio moderately higher than the imposed by the expander geometry, or Vi, the cycle efficiency can even reach higher values.

Although, an excessive under-expansion requires an expander with a larger Vi to operate efficiently.

Acknowledgements

The authors want to acknowledge all the invaluable cooperation of Rank®, the ORC manufacturer, for its support in this project. Also to thank greatly the Jaume I University for its financial support under the PhD grant PREDOC/2013/28 of 'Convocatòria d'ajudes predoctorals per a la formació de personal investigador del Pla de promoció de la investigació de la Universitat Jaume I de Castelló (Spain)'.

References

[1] Yamada N, Tominaga Y, Yoshiba T. Demonstration of 10-W_p micro organic Rankine cycle generator for low-grade heat recovery. Energy 2014; 78: 806-813.

[2] Li J, Pei G, Li Y, Wang D, Ji J. Energetic and exergetic investigation of an organic Rankine cycle at different heat source temperatures. Energy 2012; 38: 85-95.

[3] Bombarda P, Invernizzi CM, Pietra C. Heat recovery from Diesel engines: A thermodynamic comparison between Kalina and ORC cycles. Applied Thermal Engineering 2010; 30: 212–219.

[4] Chen H, Goswami DY, Stefanakos EK. A review of thermodynamic cycles and working fluids for the conversion of low-grade heat. Renewable and Sustainable Energy Reviews 2010; 14: 3059–3067.

[5] Tchanche BF, Lambrinos Gr, Frangoudakis A, Papadakis G. Low grade heat conversion into power using organic Rankine cycles – A review of various applications. Renewable and Sustainable Energy Reviews 2011; 15: 3963–3979.

[6] Wang M, Wang J, Zhao Y, Zhao P, Dai Y. Thermodynamic analysis and optimization of a solar-driven regenerative organic Rankine cycle (ORC) based on flat-plate solar collectors. Applied Thermal Engineering 2013; 50: 816-825.

[7] Franco A. Power production from a moderate temperature geothermal resource with regenerative Organic Rankine Cycles. Energy for Sustainable Development 2011; 15: 411–419.

[8] Al-Sulaiman F, Dincer I, Hamdullahpur F. Energy and exergy analyses of a biomass trigeneration system using an organic Rankine cycle. Energy 2012; 45: 975-985.

[9] Tempesti D, Fiaschi D. Thermo-economic assessment of a micro CHP system fuelled by geothermal and solar energy. Energy 2013; 58: 45-51.

[10] Zhang YQ, Wu YT, Xia GD, Ma CF, Ji WN, Liu SW, Yang K, Yang FB. Development and experimental study on organic Rankine cycle system with single-screw expander for waste heat recovery from exhaust of diesel engine. Energy 2014; 77: 499-508.

[11] Khatita MA, Ahmed TS, Ashour FH, Ismail IM. Power generation using waste heat recovery by organic Rankine cycle in oil and gas sector in Egypt: A case study. Energy 2014; 64: 462-472.

[12] Campana F, Bianchi M, Branchini L, Pascale AD, Peretto A, Baresi M, Fermi A, Rossetti N, Vescovo R. ORC waste heat recovery in European energy intensive industries: Energy and GHG savings. Energy Conversion and Management 2013; 76: 244–252

[13] Zhou N, Wang X, Chen Z, Wang Z. Experimental study on Organic Rankine Cycle for waste heat recovery from low-temperature flue gas. Energy 2013; 55: 216-225.

[14] Qiu G, Shao Y, Li J, Liu H, Riffat SB. Experimental investigation of a biomass-fired ORC-based micro-CHP for domestic applications. Fuel 2012; 96: 374-382.

[15] Pei G, Li J, Li Y, Wang D, Ji J. Construction and dynamic test of a small-scale organic rankine cycle. Energy 2011; 36: 3215-3223.

[16] Wang XD, Zhao L, Wang JL, Zhang WZ, Zhao XZ, Wu W. Performance evaluation of a low-temperature solar Rankine cycle system utilizing R245fa. Solar Energy 2010; 84: 353–364.

[17] Manolakos D, Kosmadakis G, Kyritsi S, Papadakis G. On site experimental evaluation of a low-temperature solar organic Rankine cycle system for RO desalination. Solar Energy 2009; 83: 646–656.

[18] Clemente S, Micheli D, Reini M, Taccani R. Energy efficiency analysis of Organic Rankine Cycles with scroll expanders for cogenerative applications. Applied Energy 2012; 97: 792–801.

[19] Peterson RB, Wang H, Herron T. Performance of small-scale regenerative Rankine power cycle employing a scroll expander. Proceedings of the Institution of Mechanical Engineers, Part A: Journal of Power and Energy 2008; 222: 271-282.

[20] Lemort V, Quoilin S, Cuevas C, Lebrun J. Testing and modeling a scroll expander integrated into an Organic Rankine Cycle. Applied Thermal Engineering 2009; 29: 3094–3102.

[21] Declaye S, Quoilin S, Guillaume L, Lemort V. Experimental study on an open-drive scroll expander integrated into an ORC (Organic Rankine Cycle) system with R245fa as working fluid. Energy 2013; 55: 173-183.

[22] Bracco R, Clemente S, Micheli D, Reini M. Experimental tests and modelization of a domestic-scale ORC (Organic Rankine Cycle). Energy 2013; 58: 107-116.

[23] Kang SH. Design and experimental study of ORC (organic Rankine cycle) and radial turbine using R245fa working fluid. Energy 2012; 41: 514-524.

[24] Kane M, Larrain D, Favrat D, Allani Y. Small hybrid solar power system. Energy 2003; 28: 1427–1443.

[25] Forni D, Rossetti N, Vaccari V, Baresi M, Santo DD. Heat recovery for electricity generation in industry. ECEEE, Summer Study on Energy Efficiency in Industry. Arnhem, The Netherlands; 2012.

[26] Leibowitz H, Smith IK, Stosic N. Cost effective small scale ORC systems for power recovery from low grade heat sources. Proceedings of IMECE2006, Nov 5-10, 2006, Chicago, Illinois, USA; 2006.

[27] Rank®. Castellon, Spain. Available from: www.rankweb.es [accessed 10.12.14].

[28] Lemmon E, Huber M, McLinden M. NIST REFPROP standard reference database 23. Version 8.0. User's guide. NIST; 2007.

[29] Quoilin S, Broek MVD, Declaye S, Dewallef P, Lemort V. Techno-economic survey of Organic Rankine Cycle (ORC) systems. Renewable and Sustainable Energy Reviews 2013; 22: 168–186.

[30] Erhart T, Eicker U, Infield D. Part-load characteristics of Organic-Rankine-Cycles. 2nd European Conference on Polygeneration. Tarragona, Spain; 2011.

Peris B, Navarro-Esbrí J, Molés F, Collado R, Mota-Babiloni A. Performance evaluation of an Organic Rankine Cycle (ORC) for power applications from low grade heat sources. Applied Thermal Engineering 2015; 75: 763–769.

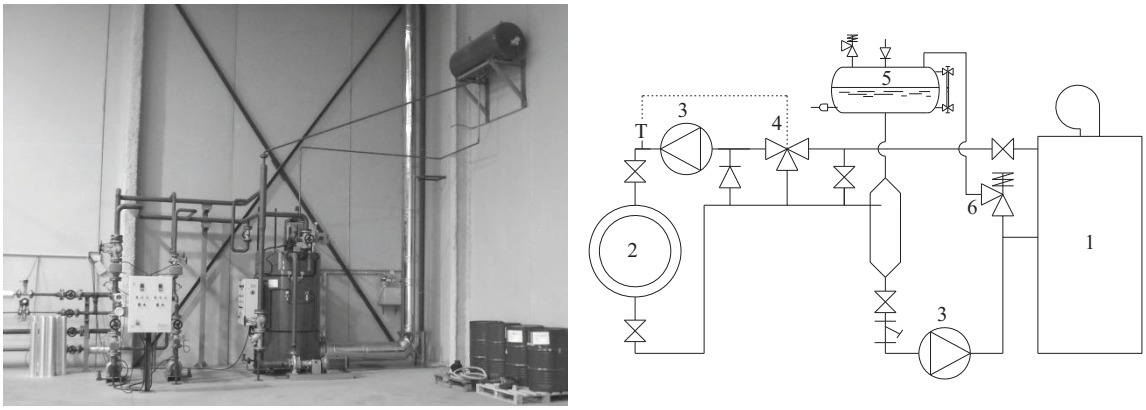

(a) (b)

Fig. 1. Heat source test bench: (a) general view of the facility, (b) basic scheme.

(a)

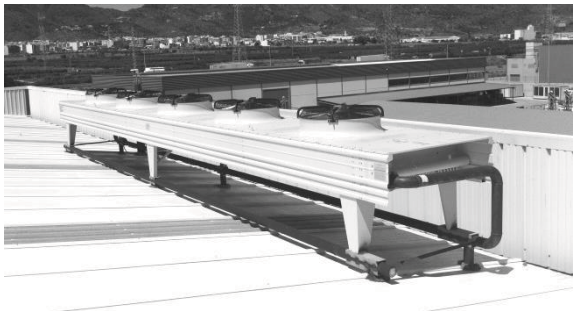

(b)

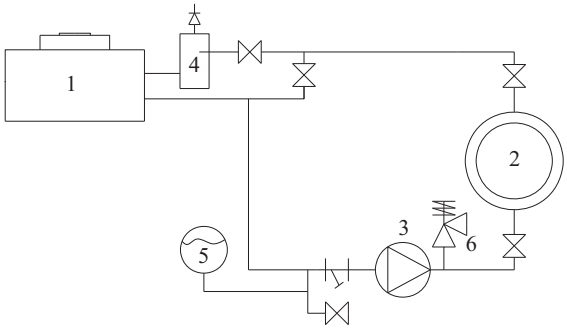

(c)

Fig.2. Heat sink test bench: (a) general view of the facility and ORC module, (b) dry cooler, (c) basic scheme.

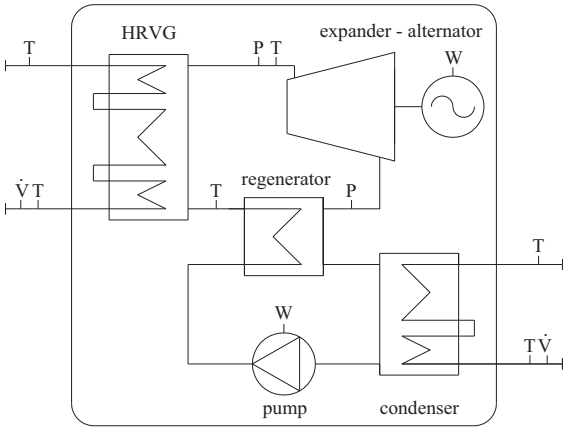

Fig.3. Regenerative ORC scheme and main parameters monitored.

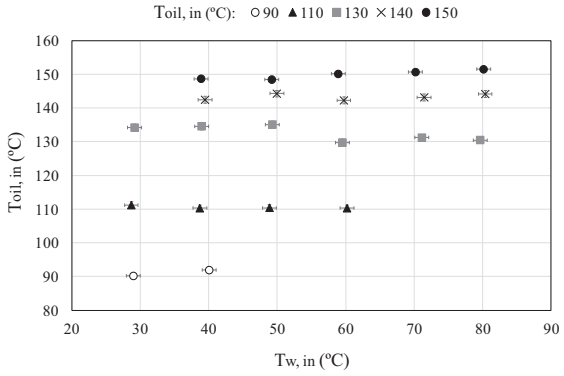

Fig.4. Operating points obtained during steady states in tests.

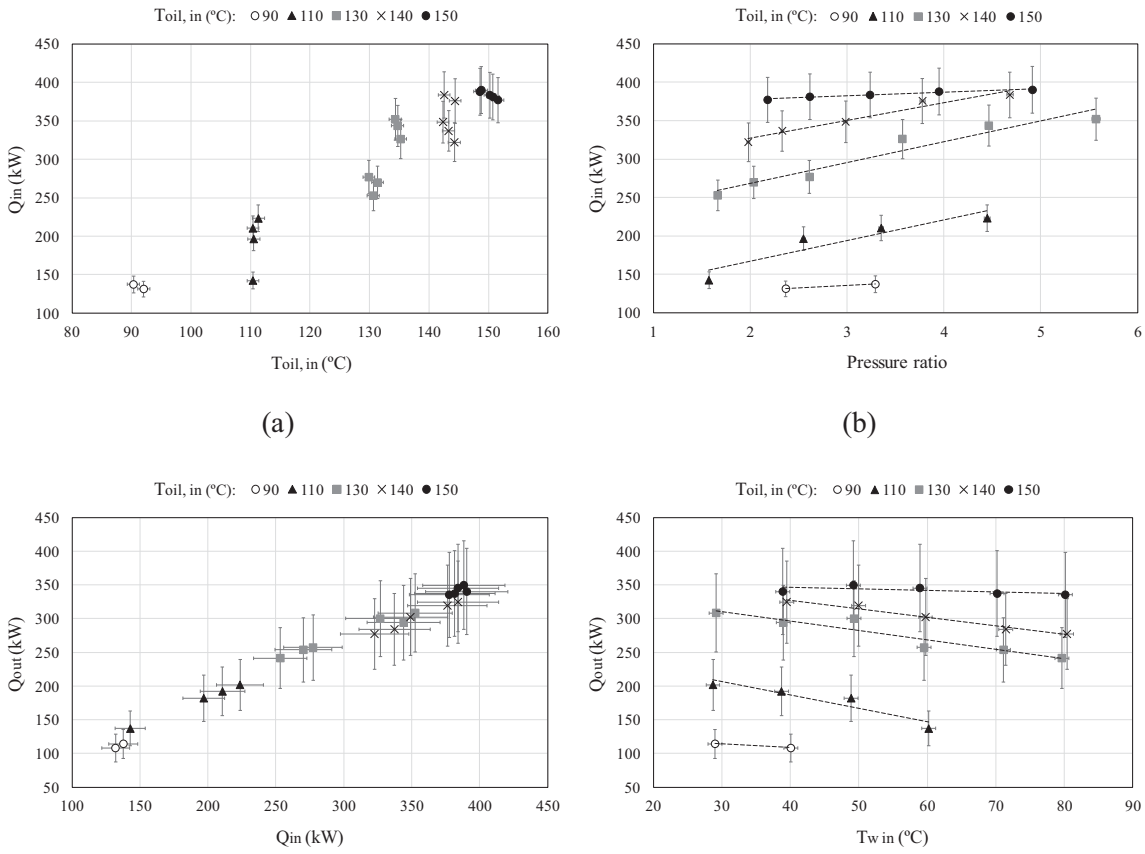

Fig.5. Thermal power characterization: (a) thermal oil inlet temperature, (b) pressure ratio, (c) useful heat, (d) hot water inlet temperature.

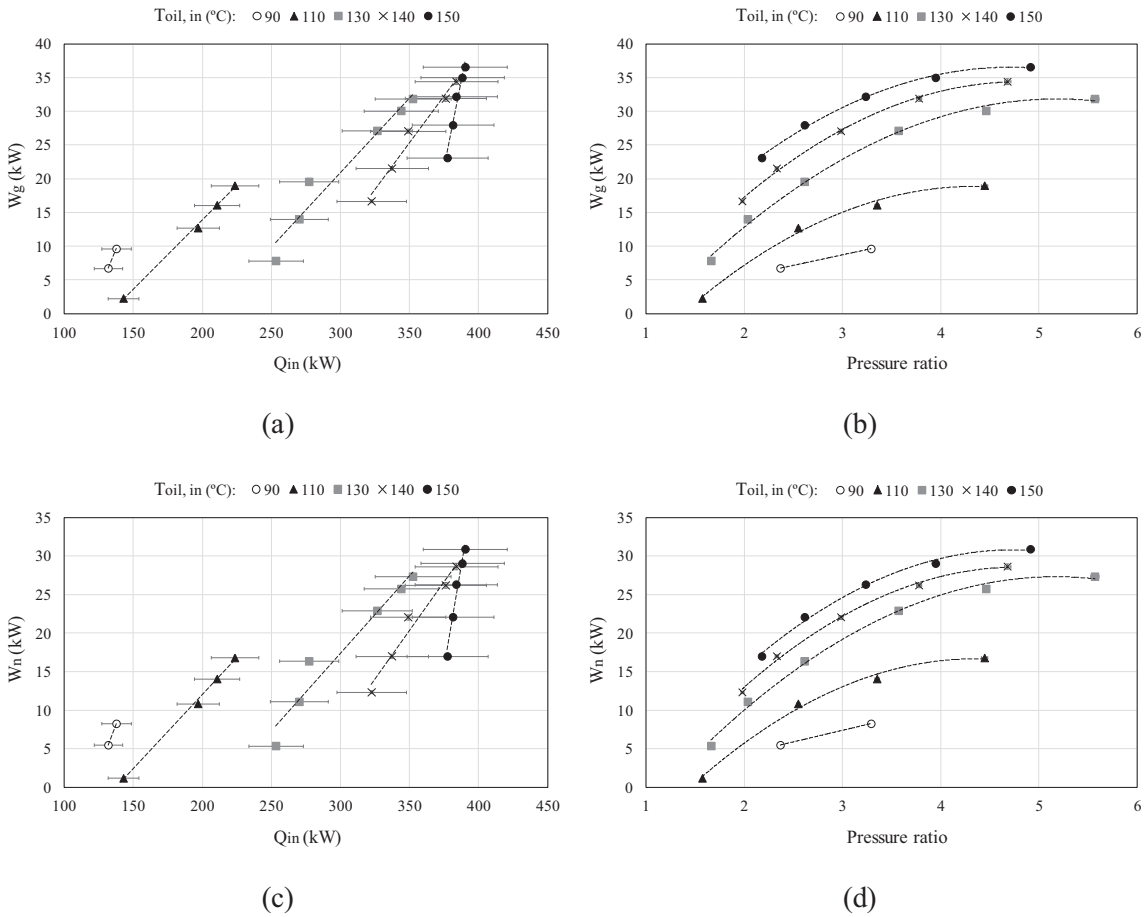

Fig.6. Electrical power characterization: (a) gross electricity with thermal input, (b) gross electricity with pressure ratio, (c) net electricity with thermal input, (d) net electricity with pressure ratio.

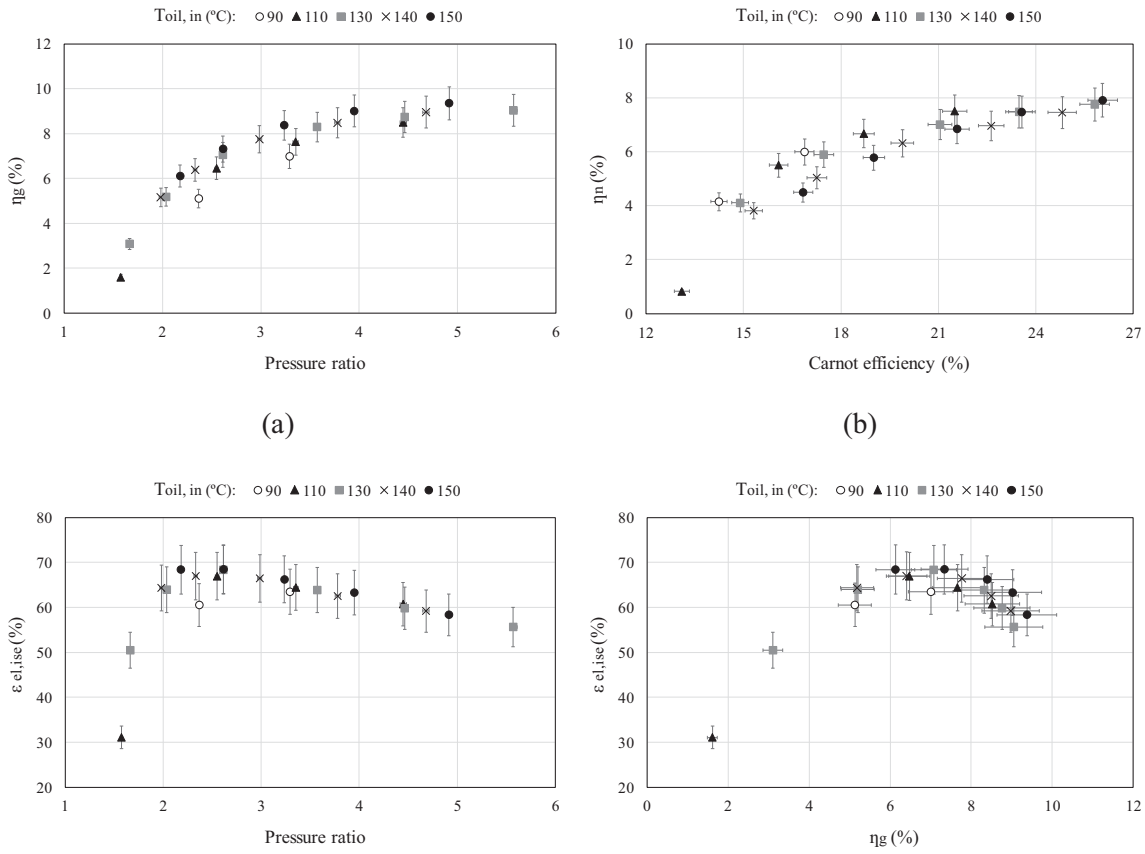

Fig.7. Thermodynamic efficiencies characterization: (a) gross, (b) net, (c) expander, (d) cycle.

Figure captions

Fig. 1. Heat source test bench: (a) general view of the facility, (b) basic scheme.

Fig.2. Heat sink test bench: (a) general view of the facility and ORC module, (b) dry cooler, (c) basic scheme.

Fig.3. Regenerative ORC scheme and main parameters monitored.

Fig.4. Operating points obtained during steady states in tests.

Fig.5. Thermal power characterization: (a) thermal oil inlet temperature, (b) pressure ratio, (c) useful heat, (d) hot water inlet temperature.

Fig.6. Electrical power characterization: (a) gross electricity with thermal input, (b) gross electricity with pressure ratio, (c) net electricity with thermal input, (d) net electricity with pressure ratio.

Fig.7. Thermodynamic efficiencies characterization: (a) gross, (b) net, (c) expander, (d) cycle.

Table 1. Rank® ORC module parameters.

Alternator rated power (kW)	45
Rated thermal power input (kW)	450
Rated thermal power output (kW)	400
ORC configuration	regenerative
Working fluid	R245fa
Expander technology	volumetric
Heat exchangers type	brazed plate
Maximum activation temperature (ºC)	170
Maximum hot water outlet temperature (ºC)	90

Table 2. Uncertainties of measured and calculated parameters.

Parameter	U
Temperature (ºC)	± 1
Pressure (%)	0.5
Thermal oil volumetric flow rate (%)	0.75
Hot water volumetric flow rate (%)	0.66
Electrical power (%)	1.20
Thermal power input (%)	7.78
Thermal power output (%)	18.77
Thermal efficiency (%)	20.39
Net electrical power (%)	1.55
Gross cycle electrical efficiency (%)	7.88
Net cycle electrical efficiency (%)	7.94
Expander electrical isentropic effectiveness (%)	7.96
Pressure ratio (%)	0.71
Carnot efficiency (%)	1.75

Table 3. Operating range of each variable obtained during tests.

Parameter	Operating range
$T_{oil,\,in}$ (ºC)	90.28 – 151.56
$T_{oil,\,out}$ (ºC)	79.92 – 127.04
$\dot{V}_{oil}$ ($m^3 \cdot s^{-1}$)	7.46E-3 – 8.12E-3
$T_{w,\,in}$ (ºC)	28.67 – 80.35
$T_{w,\,out}$ (ºC)	32.86 – 90.38
$\dot{V}_{w}$ ($m^3 \cdot s^{-1}$)	7.45E-3 – 8.24E-3
$P_{e,\,in}$ (bar)	7.25 – 22.92
$P_{e,\,out}$ (bar)	2.21 – 10.53
$T_{e,\,in}$ (ºC)	87.11 – 146.01
$T_{HRVG,\,in}$ (ºC)	48.36 – 102.15
W_g (kW)	2.29 – 36.58
W_p (kW)	1.10 – 6.10